JEB®

Journal of Environmental Biology

p-ISSN: 0254-8704 • e-ISSN: 2394-0379 • CODEN: JEBIDP

Journal website : www.jeb.co.in ★ **E-mail :** editor@jeb.co.in

Triveni Enterprises (Educational Services Set-up)

Original Research

DOI : http://doi.org/10.22438/jeb/43/1/MRN-1873

Estimation of soil organic carbon in agricultural fields: A remote sensing approach

R. Madugundu[1]*, K.A. Al-Gaadi[1,2], E. Tola[1,2], M. Edrris[1], H. Edrees[1], A. Alameen[1] and R.B. Fulleros[2]

[1]Precision Agriculture Research Chair, King Saud University, Riyadh-11451, Saudi Arabia

[2]Department of Agricultural Engineering, College of Food and Agriculture Sciences, King Saud University, Riyadh-11451, Saudi Arabia

***Corresponding Author Email :** rmadugundu@ksu.edu.sa

Received: 27.02.2021 *Revised*: 10.06.2021 *Accepted*: 03.08.2021

Abstract

Aim: In view of the importance of Soil Organic Carbon (SOC) in agricultural management, a study was conducted to develop a digital SOC map using remotely sensed spectral indices. The present study was conducted on the Tawdeehiya Farms, located in the central region of Saudi Arabia between Al-Kharj and Haradh cities.

Methodology: Landsat-8 (L8) and Sentinel-2 (S2A) satellite images were used for the characterization of SOC stocks in the topsoil layer (0-10 cm) of the experimental fields. Soil samples were randomly collected from six (50 ha each) agricultural fields and analyzed in the laboratory for SOC (SOC_A) following Walkley and Black method. While, vegetation indices (VI), such as the Normalized Difference Vegetation Index (NDVI), NDVIRedEdge, Enhanced Vegetation Index (EVI), Bare Soil Index (BSI), and Reduced Simple Ratio (RSR) were computed and subsequently used for the development of SOC prediction models.

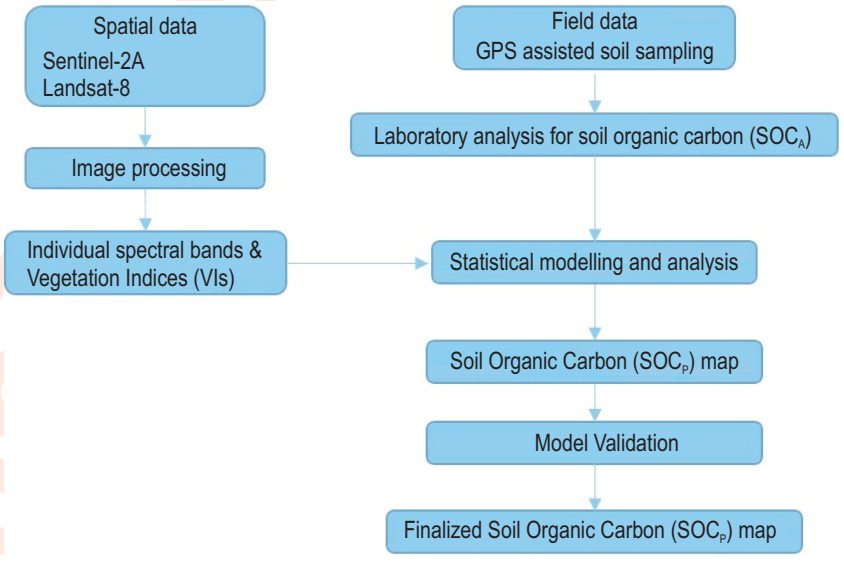

Results: Univariate linear regression technique was employed for the recognition of a suitable band/VI for SOC (SOC_P) mapping. The SWIR-1 band of both L8 (R^2 = 0.86) and S2A (R2 = 0.77) data was promising for predicting SOC with 16% (S2A) and 18% (L8) of BIAS.

Interpretation: The NDVI and BSI (for L8 data) and BSI and RSR (for S2A data) were found most suitable VI in the prediction of SOC. The R^2 values of linear regression models were 0.68 (BSI) and 0.78 (RSR), indicating that nearly 68% and 78% of the SOC could be predicted through L8 and S2A datasets, respectively.

Key words: Mapping, Satellite imagery, Soil organic carbon, Univariate analysis, Vegetation indices

How to cite : Madugundu, R., K.A. Al-Gaadi, E. Tola, M. Edrris, H. Edrees, A. Alameen and R.B. Fulleros: Estimation of soil organic carbon in Agricultural fields: A remote sensing approach. *J. Environ. Biol.*, **43**, 73-84 (2022).

Introduction

Reliable data and characterization of soil properties are prerequisites for the sustainable management of agricultural fields. Of which, soil organic carbon (SOC) content is considered as one of the essential indicators of soil nutrients and soil biota (Shibu *et al.,* 2006). It also enhances the soil structure and water storage capacity of a field (Schoonover and Crim, 2015). In terms of environmental quality, the increase in SOC content helps in the mitigation of greenhouse gases (Lal, 2004). Thus, quantitative measurements and mapping of SOC are essential for agricultural management, agro-forestry, and terrestrial sequestration of atmospheric carbon (Man *et al.,* 2017). Conventional methods used for the estimation of SOC (collection and analysis of soil samples) are laborious, time-consuming, and expensive. On the other hand, SOC determined by conventional methods may not reflect its accurate estimates (Jaber *et al.,* 2012; Shit *et al.,* 2016).

Soil organic carbon varies spatially even within small areas (Baruah *et al.,* 2020), hence, it is also practically impossible to sample large areas and achieve continuous data coverage. Therefore, estimation of SOC concentration in agricultural soils at an acceptable level of accuracy is important, especially in the case when SOC exhibits strong spatial dependence and its measurement is a time and labor-intensive procedure. Hence, there is an urgent need to develop rapid and inexpensive soil characterization techniques to support many important applications, such as precision agriculture. Alternatively, SOC can be predicted using spectroscopy and satellite remote sensing techniques through the recorded spectral characteristics. To cover large areas of spatial datasets for rapid *in-situ* monitoring of SOC and its site-specific management, satellite images were widely used (Kooistra *et al.,* 2003; Stevens *et al.,* 2013). Most of the previous studies have adopted either a qualitative (Stoner and Baumgardner, 1981) or a quantitative (Ben-Dor and Banin, 1995) approach.

Advanced remote sensing (RS) and GIS systems provide a viable alternative for routine soil analysis, especially for the quantitative measurements of SOC. Recent improvements in the use of multispectral remote sensing techniques and significant progress in the analytical software programs have become attractive for SOC mapping by using remotely sensed images scanned by various satellites (Landsat, Sentinel, ASTER, etc). It is also considered a rapid, non-destructive, and cost-effective method for estimating the concentrations of SOC in agricultural soils. Moreover, a wide range of soil parameters was determined by assessing the spectral reflection from the soils of agricultural fields in the visible-near infrared-short wave infrared (VIS-NIR-SWIR) regions (Stevens *et al.,* 2013).

On the other hand, Vegetation indices (BSI, NDVI, EVI, etc) have been widely used in the prediction of SOC with the use of machine learning methods (Mondal *et al.,* 2017; Bhunia *et al.,* 2019) such as random forest (RF), partial least squares regression (PLSR), support vector machine (SVM), and artificial neural network (ANN) and linear regression models (Mallick *et al.,* 2020) employed on satellite images such as Landsat (Viscarra-Rossel and Bouma, 2016; Kumar *et al.,* 2016), Sentinel-2 (Wang *et al.,* 2021; Dvorakova *et al.,* 2021), etc. Many studies have been conducted to investigate the characteristics of soil spectral reflection in regions of moderate to high soil fertility levels, but studies in low-fertility soils are still limited in the Arab region, such as Saudi Arabia.

As an example, as part of agroecological exploration of the Arabian Peninsula, De Pauw (2002) created a SOC map for the entire Arabian Peninsula. At larger scale, Schillaci *et al.* (2016) and Darwish and Fadel (2017) prepared SOC maps for the Mediterranean region/Arab region. At the regional scale, Tola *et al.* (2018, 2019) assessed the SOC concentration in the parts of Al-Kharj region of Saudi Arabia, with special emphasis on the long-term impact of tillage on the soil organic carbon. Another study by Mallick *et al.* (2020) was developed SOC prediction models for Asir Province, Saudi Arabia. Most of these SOC studies have been focused on areas with vegetation growing over the soil surface (forest and cropland), and there have been few reports regarding bare cropland topsoil for different soil types as well as land uses.

As the prediction accuracy of models depend on local conditions, the present study aimed to characterize the soil organic carbon (SOC) of low-fertility agricultural fields in the parts of Al-Kharj region, Saudi Arabia, using"free-of-cost" remotely sensed images, Landsat-8 (L8) and Sentinel-2 (S2A). Commonly used linear regression models were employed to link the spectral data of topsoil (30 cm). In light of the above, this study was conducted with the aim to assess the relationship between laboratory estimated SOC (SOC_A) and the spectral reflectance data scanned by S2A and L8 sensors/satellites; to develop linear regression models for the prediction/mapping of SOC concentration in agricultural soils: and to map and characterize the soil organic carbon of experimental fields for better management.

Materials and Methods

Study Area: The experimental work was carried out in selected agricultural fields in Tawdeehiya Farms located 250 km southeast of Riyadh, the capital city of Saudi Arabia. The farm is located within the coordinates of 24° 11' 00" N and 48° 56' 14.6" E (Fig. 1). An area of 1500 m^2 was allocated on the farm for this study. The farm experiences moderate to a hyper-arid climate with hot summers (40 ± 2°C) and cold to moderate winters (15 ± 3 °C), with a mean air temperature of 35°C and approximately annual rainfall of 90 mm, most of which occurred from November to February. The soil of the study area was mainly sandy loam with mild alkalinity, with a pH of 7.58 and a soil electrical conductivity (EC) of 2.36 dS m^{-1}. The observed wilting point, field capacity, and saturated hydraulic conductivity values were 7 mm, 14 mm, and 3.6 m s^{-1}, respectively. The terrain of study fields was almost flat with slight undulations where the elevation ranged from 329 m to 453 m. The major crops cultivated on the farm were alfalfa, Rhodes grass, corn and carrot.

Soil sampling: A field survey was carried out on 26 March 2017 and a total of 49 soil samples were collected from the topsoil layer (0 to 10 cm). A hand-held GPS receiver (Trimble GeoXH) was used to locate the pre-defined sampling points (Fig. 1). The random sampling method was adopted and the sample locations were selected based on the apparent variation in land use cover, topography, and soil texture. Subsequently, the collected soil samples were air-dried and subsequently, analyzed in laboratory for soil organic carbon (SOC_A) content.

Soil Organic Carbon (SOC) mapping: The flow chart of procedures involved in SOC mapping is given in Fig. 2. The collected soil samples were analyzed for SOC (SOC_A). The vegetation indices developed from the satellite images were utilized to develop empirical models through regression techniques.

Laboratory analysis-SOC: Widely used Walkley-Black (1934) titration method was employed for the estimation of the SOC_A. Initially, the collected soil samples were air-dried and sieved (<2 mm) to remove plant debris and large root matter. Thereafter, the SOC_A was quantified as given in Eq. 1.

$$\text{Organic Carbon (\%)} = N \times (B-S) \times 0.003 \times \frac{100}{\text{Wt. of soil}} \quad \text{.....(1)}$$

where, N is the normality of standard ferrous ammonium sulphate: B and S are the amount of ferrous ammonium sulphate utilized during titration for the blank and soil sample, respectively. Subsequently, the obtained SOCA (%) values were transformed into unit values (g C kg^{-1}).

Satellite data and image analysis: A total of four cloud-free images of Sentinel-2A (S2A) and Landsat-8 (L8) were downloaded from the USGS portal (https://earthexplorer.usgs.gov/) corresponding to the field inventory of soil sample collection (i.e. 24 March 2017). Details of the acquired S2A and L8 images are provided in Table 1. The Q-GIS (Ver. 2.18) software program was used to perform image analysis. The acquired L8 and S2A images were pre-processed for surface reflectance. Determination of reflectance value was achieved using the "semi-automatic Classification Plugin (SCP)" of the Q-GIS. Subsequently, the vegetation indices (VI) were computed using the standard equations (Table 2) applied on L8 and S2A spectral bands. The obtained SIs were assessed against the lab-determined SOC (i.e. SOC_A). A stepwise linear regression approach was used in the identification of a suitable band or index for predicting the soil organic carbon (SOC_P).

Modelling and prediction of SOC_P: To obtain the predicted SOC (SOC_P) map of the experimental farm, a regression analysis based empirical equation was generated with S2A and L8 datasets against the SOC_A. During the process, the relationship between the spectral reflectance of S2A and L8 datasets and the SOC_A was assessed using the SPSS (Ver. 20) statistics software program (IBM, New York, USA). Of the collected samples, 60% was used for the model development and the remaining 40% was utilized for model accuracy assessment. The best-fit model was tested for its strength by the coefficient of determination (R^2), histograms of the residuals, and normal probability plots. To generate the SOC_P map, the obtained empirical model was applied on the targeted spectral index (SI) using raster calculator tool of ArcGIS (Ver. 2010). Subsequently, the accuracy of the obtained SOC map was evaluated using cross- validation/ model performance/ statistical methods by comparing the SOC_A values to the SOC_P values.

Leave-one-out validation analysis: Prediction accuracy was evaluated employing the coefficient of determination (R^2), root mean square error (RMSE), and bias (Bias). The model with the lowest RMSE and highest R^2 values was considered to be the most applicable or ideal model (Jaber *et al.,* 2012).

$$\text{RMSE} = \sqrt{\frac{\sum_{i=1}^{n} (\hat{y}_i - y_i)^2}{n}} \quad (2)$$

$$\text{Bias} = \frac{\sum_{i=1}^{n} \hat{y}_i - y_i}{n} \quad (3)$$

where, $\hat{y}i$ is the estimate and yi is the observed value.

Results and Discussion

Laboratory analyzed soil organic carbon (SOC_A): Collected samples were subjected to laboratory analysis for SOC_A and the results are summarized in Table 3. The SOC_A varied from 0.62 to 14.71 g C kg^{-1} with a mean value of 7.8 g C kg^{-1}.The studied bare soil fields showed a 59% coefficient of variation in the SOC_A. The elevation differed east to west from 364 to 401m. Spatial irregularities were assumed to be non-influential and the spatial distribution of SOC content was assessed based on the bare soil and vegetation condition of the study fields.

Table 1: Details of sensors used and Acquired Images

Sensor	Path/Row/Scene-ID	Date of overpass
Sentinel-2A (L1C)	T38QRM	24 March 2017
Landsat-8 (L1T)	165/44	29 March 2017
Sentinel-2A (L1C)	T38QRM	03 April 2017
Landsat-8 (L1T)	165/45	14 April 2017

Table 2: Description of Spectral Indices (SIs) used in the study (*Landsat-8; #Sentinel-2A)

Spectral Indices	Equations	Reference
NDVI*	NDVI = (NIR-Red)/(NIR+R)	Rouse *et al.* (1934)
NDVIRedEdge#	NDVIRE = (NIR-RedEdge)/(NIR+ RedEdge)	Eitel *et al.* (2011)
Bare soil index	$BSI = \frac{[(SWIR + Red)-(NIR + Blue)]}{[(SWIR + Red)+(NIR + Blue)]}$	Jamalabad and Akbar (2004)
Reduced simple ratio	$RSR = \frac{NIR}{Red}\left(1-\frac{SWIR-SWIR_{min}}{SWIR_{max}-SWIR_{min}}\right)$	Brown *et al.* (2000)
Enhanced Vegetation Index	$EVI = 2.5\ \frac{NIR-Red}{NIR + 6 \cdot Red - 7.5 \cdot Blue + 1}$	Huete *et al.* (2002)

Table 3: Descriptive Statistics of SOC_A (g C kg^{-1}) and the SIs Generated from Landsat-8 and Sentinel-2A datasets

Min	Max	Mean	Range	Stdev.	SE	CV (%)
0.62	14.71	7.8	44.1	3.91	0.41	58.7

Table 4: Sensor wise Developed prediction models for SOC (y= SOC_P) Mapping

Sensor	X factor	Model	UA (%)	PA (%)
Landsat-8	SWIR-1	y = (-10.956*X)+3.074	59.7	66.2
	NDVI	y = (0.3445*X)+0.2141	32.9	42.6
	BSI	y = (12.68*X)-0.078	74.2	77.4
	RSR	y = (0.4861*X)+0.1604	54.9	64.2
Sentinel-2A	SWIR-1	y = (-12.636*X)+3.344	54.2	59.7
	$NDVI_{RE}$	y = (2.4058*X)+11.49	78.2	84.1
	BSI	y = (0.4861*X)+0.1604	52.6	48.9
	RSR	y = (2.4058*X)+78.12	69.8	74.2

Table 5: Performance of the SOC prediction models

Parameters	Landsat-8 (L8)			Sentinel 2A (S2A)		
	R^2	Adj. R^2	SE of Estimate	R^2	Adj. R^2	SE of Estimate
SWIR-1	0.64	0.59	0.42	0.67	0.62	0.47
BSI	0.72	0.68	0.66	0.62	0.44	0.59
NDVI or $NDVI_{RE}$	0.34	0.31	0.59	0.58	0.52	0.61
RSR	0.22	0.17	0.62	0.83	0.78	0.55

Relationship between SOC_A and satellite data: The spectral reflectance of bare soil images from S2A and L8 are given in Fig. 3.The results showed the variance of spectral reflections in the ultraviolet and near-infrared wavelength ranges of the topsoil and the dynamics in the electromagnetic spectrum. The spectral reflectance (0.16 – 0.44 %) from the L8 bands was two folds higher than the S2A reflectance (0.04 – 0.24 %). Moreover, there was a fall/decrease in reflectance at the NIR band of S2A compared to L8. Similarly, the SWIR-2 band of L8 showed a decreasing trend compared to S2A. The mean values of NDVI, BSI, RSR and EVI of L8 data were 0.08, 0.98, 0.17, and 0.35, respectively. For S2A data, the mean values of NDVI, BSI, RSR and EVI were 0.09, 1.02, 0.47, and 0.67, respectively. Individual maps of VIs are illustrated in Fig. 4 and 5 for L8 and S2A datasets, respectively.

The NDVI of L8 image exhibited low values of 0.05 to 0.13 as the image was captured at bare soil condition (mean BSI =

Table 6: Cross Validation of SOC Prediction Model Performance

Parameters	Landsat-8			Sentinel – 2A		
	SWIR-1	BSI	NDVI	SWIR-1	BSI	RSR
Mean (g C Kg^{-1})	13.42	13.75	13.59	12.72	13.15	12.94
R2 RMSE	0.860	0.792	0.723	0.765	0.863	0.814
(g C Kg^{-1})	2.612	2.141	2.761	1.903	2.341	2.122
RMSE (%)	11.21	9.95	10.56	10.11	9.17	11.14
Bias (%)	15.92	16.21	16.06	13.54	11.12	15.33

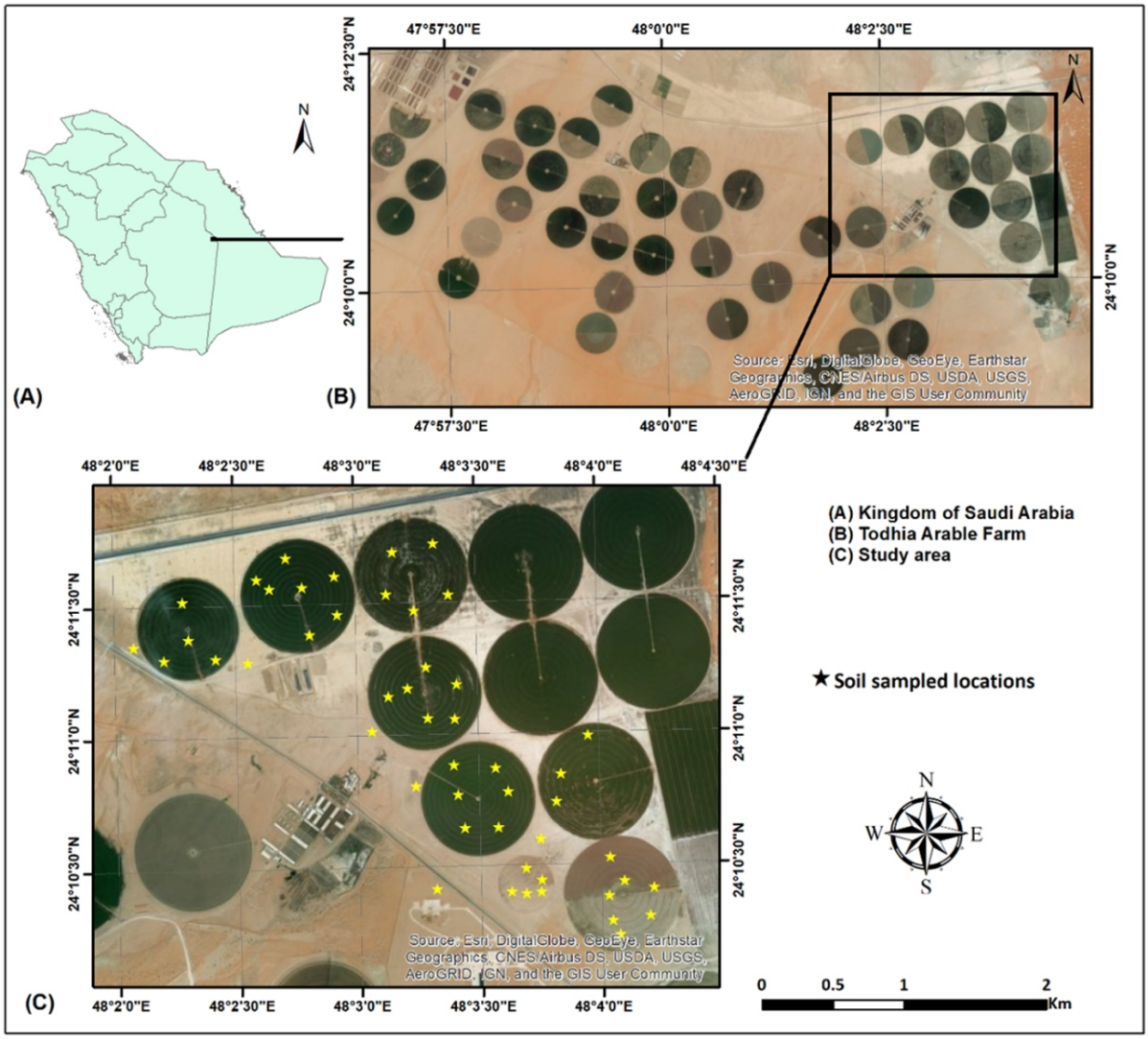

Fig. 1: Location of the experimental field overlaid by the sampled locations.

0.98) represented by a low intensity of vegetation cover. Also, the high values of RSR (0.38 - 1.12) and EVI (0.22 - 0.50) confirmed the no-vegetation condition of the field. For the S2A dataset, the values of studied indexes were slightly higher than those of the L8 dataset. Variation between the NDVI of L8 and the $NDVI_{RE}$ of S2A was negligible (0.01). The deviation, however, was more in BSI

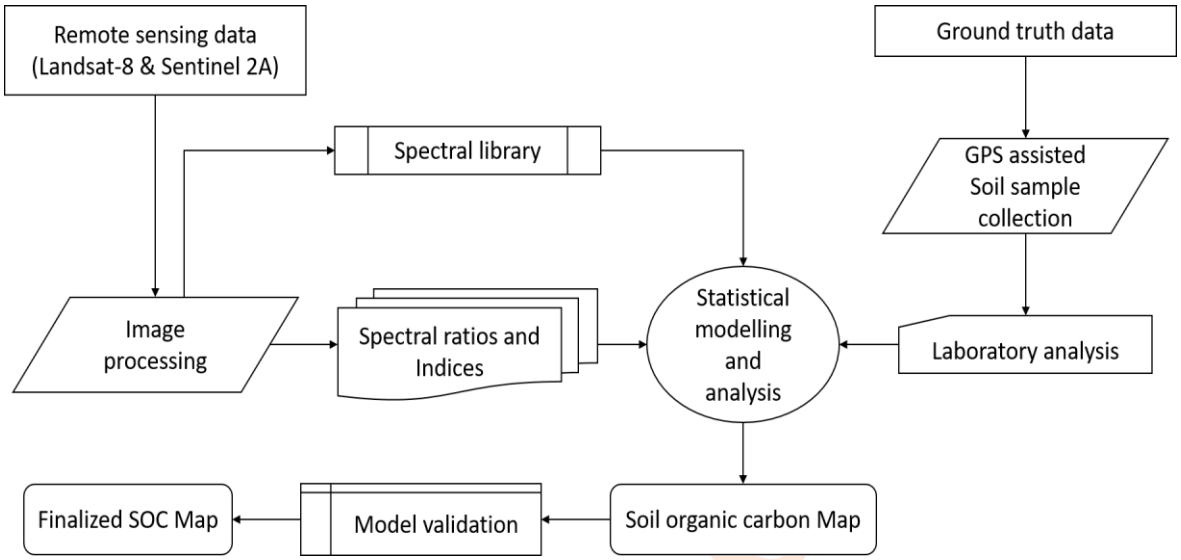

Fig. 2: Methodological flowchart - soil organic carbon mapping.

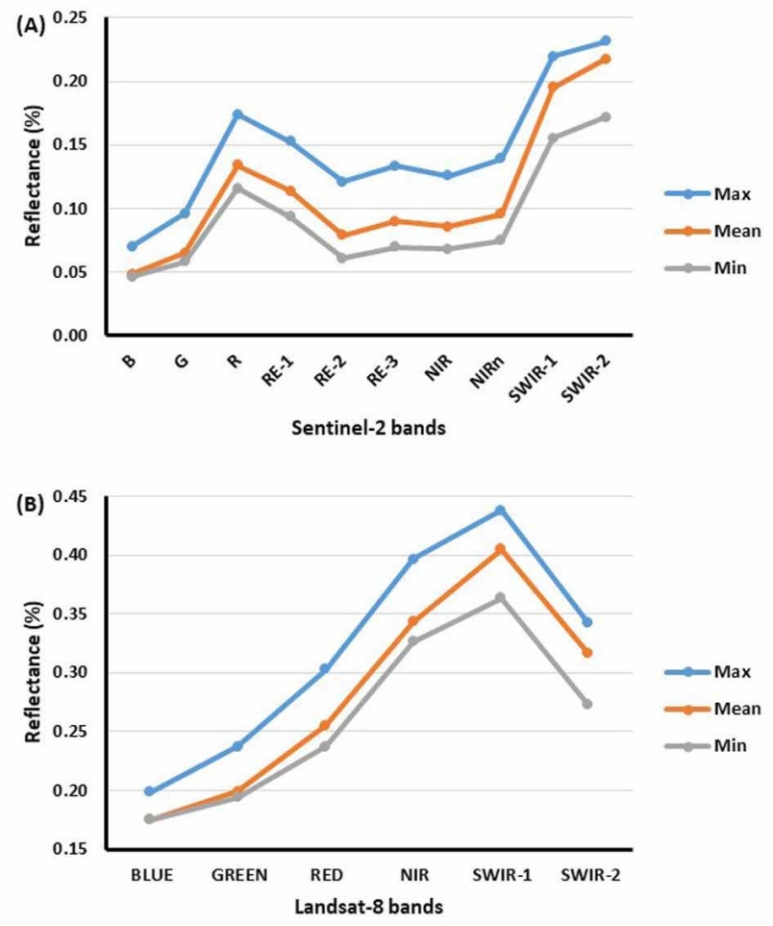

Fig. 3: Spectral reflectance of soil samples: Sentinel-2 (a) and Landsat-8 (b).

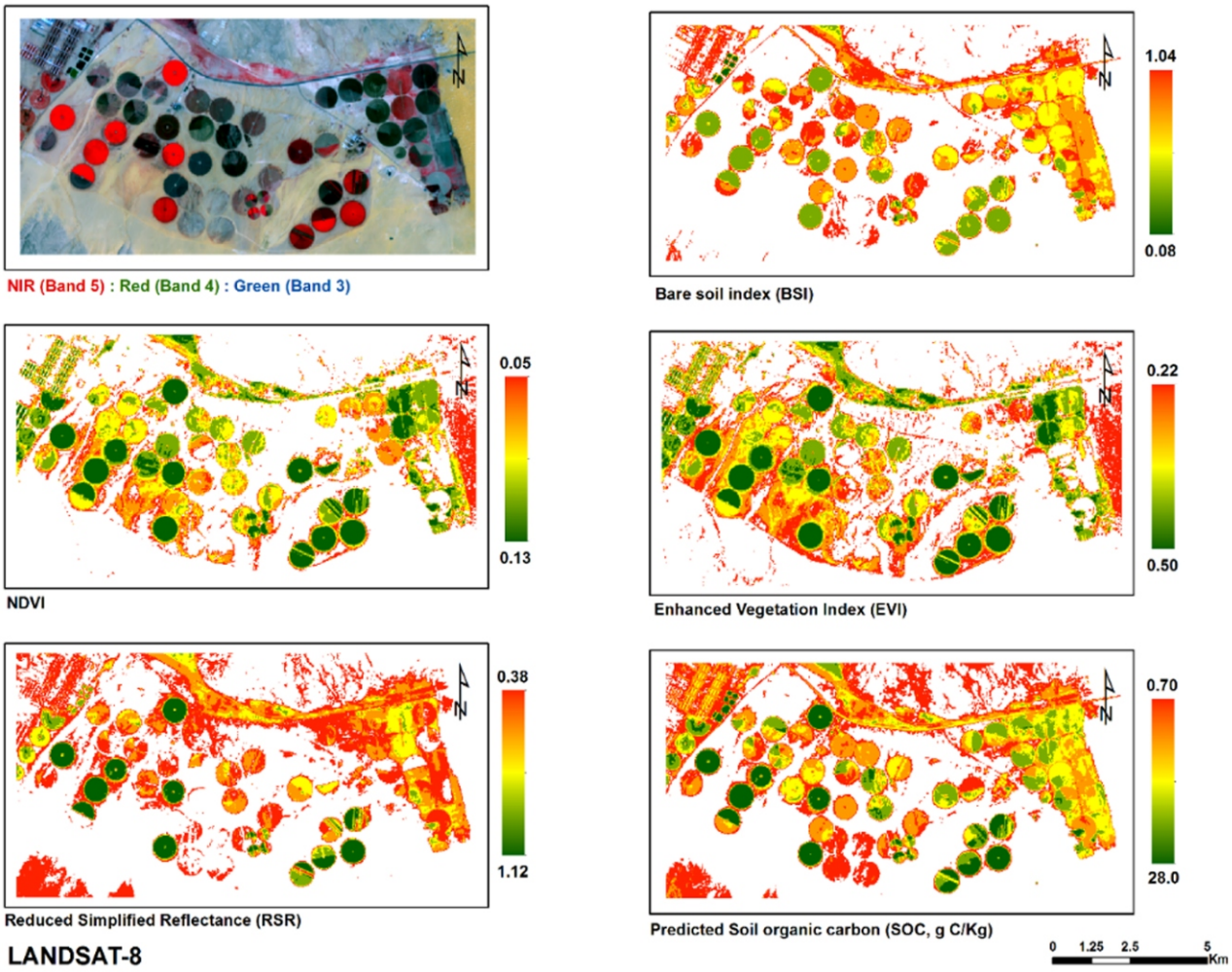

Fig. 4: Vegetation indices generated from Landsat-8 data.

(0.04), followed by RSR (0.30) and EVI (0.32). The regression (linear) analysis between the SOC_A and the vegetation indices (VI) was performed and the generated empirical models are presented in Table 4. The user's accuracy (UA) and the producer's accuracy (PA) of the prediction layers were assessed. The SWIR-1 band was found better in predicting the SOC for both the L8 and S2A datasets. In the case of vegetation indices, the BSI and the NDVI performed well with L8 data, while the $NDVI_{RE}$ and the RSR did the same with S2A data (Table 4).

SOC prediction models – performance: The performance of the generated SOC_P models was statistically assessed (Table 5). Out of four VI studied, two VI from each of the L8 and S2A datasets showed significant correlation between the SIs and the SOC_A, with R^2 values ranging between 0.38 and 0.78. For the L8 dataset, the BSI and the NDVI were found more suitable for predicting SOC. However, for S2A dataset, the BSI and RSR were identified most sensitive VI for predicting SOC. The NDVI and BSI of L8 were found more accurate (P< 0.0001) for predicting the SOC. However, in the case of S2A, the BSI and RSR showed a statistically significant relationship with the observed SOC (P< 0.0001), as given in Table 5. Conversely, high BSI values were associated with bare soil fields or dried vegetation with low NDVI values. The spatial distribution of SOC observed in the experimental farm was determined with low to medium SOC_P values. Details of the model performance analysis are presented in Table 5. The R^2 values of linear regression models were 0.68 (BSI) and 0.78 (RSR), indicating that nearly 68% and 78% of the SOC could be predicted through L8 and S2A datasets, respectively, through BSI.

The correlation between the predicted and the observed SOC values revealed that the S2A dataset exhibited the best correlation with BSI (R2=0.863, P<0.0001) compared to those exhibited by the L8 dataset (R2 = 0.792, P<0.001). The model accuracy of 64% (L8) and 72% (S2A) were achieved in the prediction of SOC. RMSE (%) of predictive model from SWIR band was between 11.21 (L8) and 10.21 (S2A), while BSI

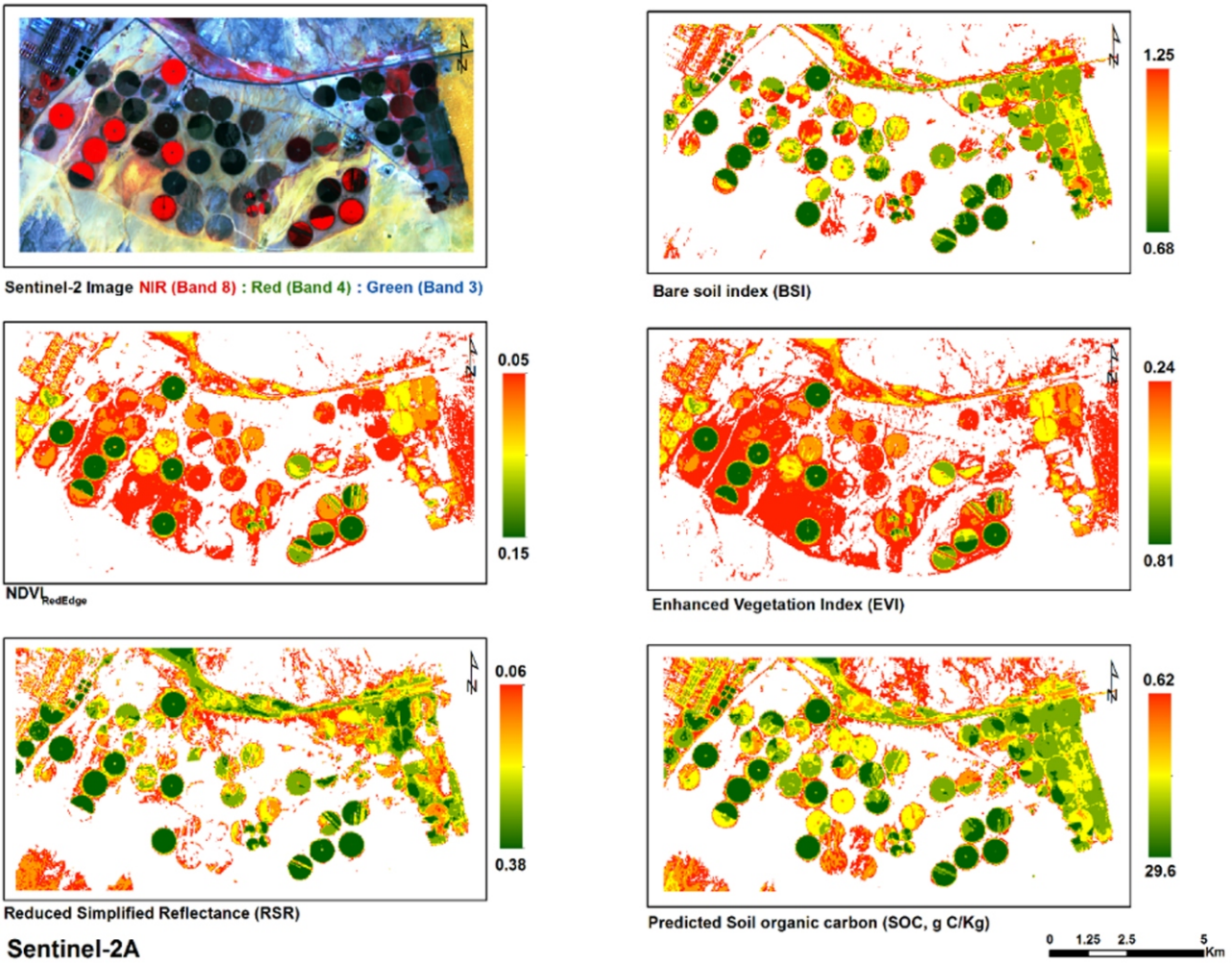

Fig. 5: Vegetation indices generated from Sentinel-2 data.

exhibited RMSE values of 9.95% and 9.17% for L8 and S2A, respectively (Table 6). Performance analysis of SOC_A and SOC_P obtained using VI (Fig. 6 and Fig. 7) showed the goodness of fit, and the test results revealed no significant difference between the observed and the predicted SOC at 0.05 significance level. The results also indicated an increase in the SOC with the increase in NDVI and a decrease in BSI. The maximum recorded value of digital SOC map was 28 g C kg^{-1} and 29.6 g C kg^{-1} for L8 and S2A datasets, respectively. While negligible SOC values (~0.7 – 1.5 g C kg^{-1}) were recorded in the farm areas covered by non-agricultural activities (sand area and discontinued pivots) showed negligible SOC values.

Moreover, this study investigated medium (30-m and 10-m) resolution satellite images with varying bandwidths. Most of the earlier studies (Shit *et al.,* 2016; Bhunia *et al.,* 2016), succeeded by integrating field observations to measure digital soil maps. The spectral reflectance of a certain field can vary with the nature of soil characteristics, such as colour, nutrient holding capacity, and fertilizer assimilation, turn-over of nutrients, etc. (Ismail and Yacoub, 2012). For example, in this study, the NDVI was found to be one of the most important features explaining the SOC variability as reported by Wang *et al.* (2018) and Nabiollahi *et al.* (2018). It is because of the dependency of SOC on vegetation cover, NDVI has frequently been used as a predictor for mapping SOC. Direct correlation between spectral indices and SOC is of great importance in predicting SOC, which plays a vital role in controlling many vital soil properties. Hence, this aimed to explore the ability of spectral bands and vegetation indices in predicting SOC. The S2A data (R^2 = 0.68, RMSE = 0.26%) showed significantly better results in terms of SOC prediction than L8 (R^2 = 0.65, RMSE = 0.28%). These results are consistent with the studies of Castaldi *et al.* (2019) and Rosero-Vlasova *et al.* (2017). Moreover, the generated SOC maps were validated using similar reference field observations (Leave-one-out). Which corroborate with the studies of (Kumar *et al.* (2016); Mondal *et al.* (2017) and Bhunia *et al.* (2016, 2019). The model performance indicators (RMSE and BIAS) also confirmed a significant

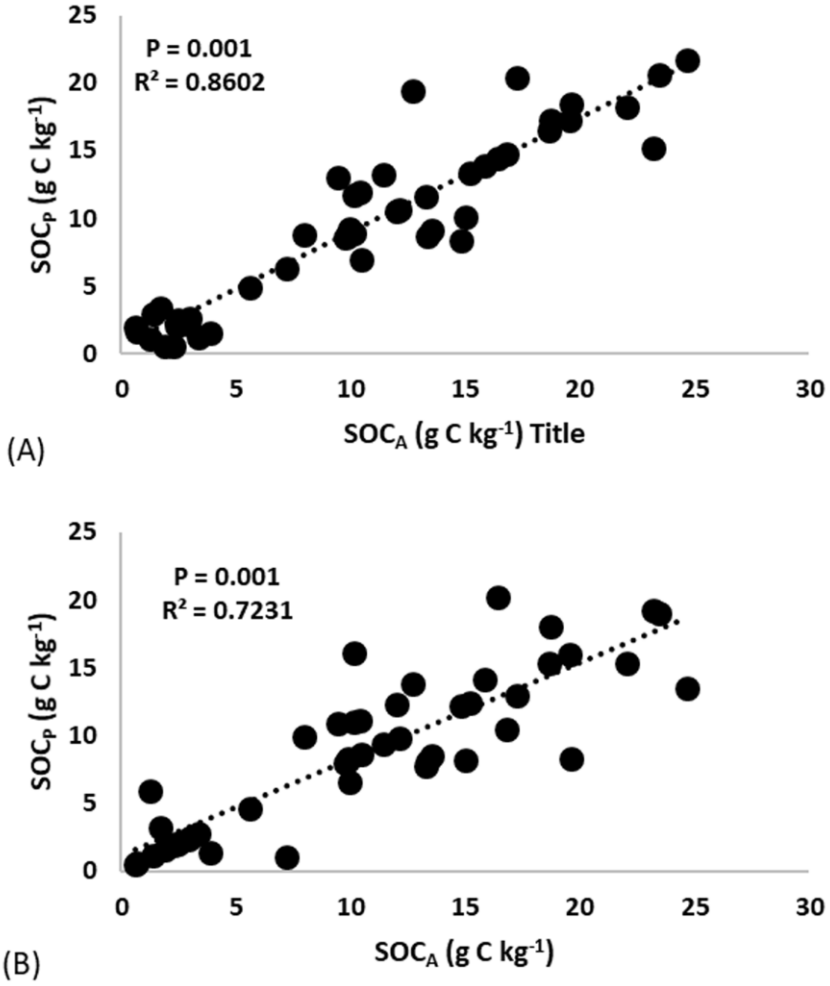

Fig. 6: Scatter plot between SOC_A and SOC_P obtained from spectral indices of Landsat-8; (A): SOC_P predicted using SWIR-1 band and (B) SOC_P predicted using BSI.

relationship between VIs and SOC. In this study, linear relationships between the SWIR-1 band, VI from the L8 and S2A satellite data were observed against the SOC_A and were confirmed with a similar study by Wang *et al.* (2021). The analysis of S2A data showed that the two SWIR broad bands centered at 1610 and 2190 nm are sufficient to satisfactorily predict SOC content, as a result, high values of BSI and low RSR areas were associated with low SOC areas, and vice versa. The potential of SOC prediction models generated in this study varied with the R^2 values of 0.86 and 0.77 for L8 and S2A datasets.

In the case of L8 data, the SOC prediction model generated in this study was performed well compared to R^2 values (0.65 to 0.78) as earlier reported by Bouasria *et al.* (2020), Mohamed *et al.* (2020), and Mallick *et al.* (2020). Whereas, the models developed from S2A showed better performance (R^2 = 0.77) than the reported values (R^2 =0.25) of Zhou *et al.* (2021) and (R^2 =0.54) by Dvorakova *et al.* (2021) but not as superior (R^2 = 0.85) to the study of Wang *et al.* (2021). In some fields that were classified as 'bare soil' (NDVI < 0.25) and consequently, the lowering of spectral reflectance in the red and red edge bands was probably due to the influence of crop residues on these wavelengths highly sensitive to vegetation. In addition, the presence of crop residues consistent presence of green or dry vegetation (> 20%) can strongly affect the spectral reflectance (Bartholomeus *et al.,* 2011), and consequently, influence the prediction accuracy of soil properties. Although, L8 and S2A imagery has been able to separate pure soils from soils with crop residues by using spectral unmixing techniques, which was not attempted in this study.

Limitations of the study: Even so, some studies on soil property monitoring using S2A as a single data source have overcome many problems and has achieved certain results (Wang *et al.,*

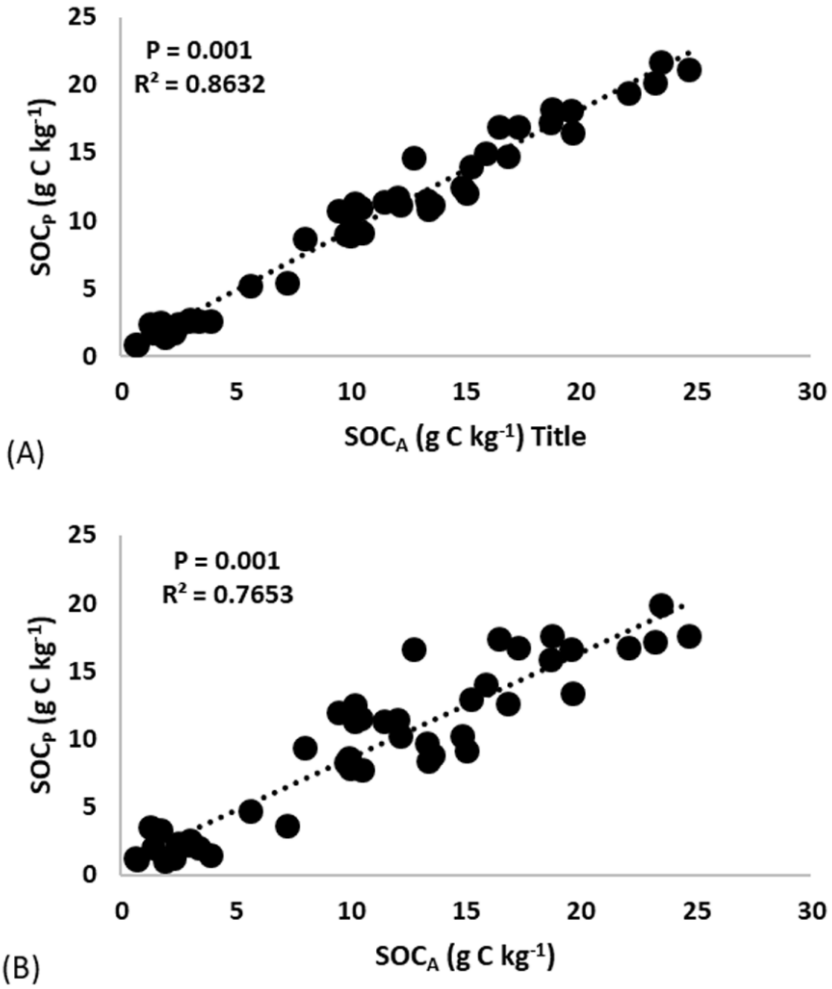

Fig. 7: Scatter plot between SOC_A and SOC_P obtained from spectral indices of Sentinel-2A; (A): SOC_P predicted using BSI, and (B) SOC_P predicted using SWIR-1 band.

2021), and the verification results are consistent with the conclusions of this study, *i.e.,* S2A can monitor soil properties, and it is expected to develop the potential for retrieving soil properties. It should be noted that there are still some limitations in the present study. First, space-borne data are controlled by the data acquisition condition, which mainly associates with atmospheric attenuation and plant litter, and the acquisition time must be as close as possible to the sampling time. Second, the effect of soil moisture and soil texture on SOC prediction was not considered in this study, as they were assumed to be relatively homogeneous. Third, the simultaneous existence of large bare tilled agricultural fields and high-quality remote sensing images is an important prerequisite for replicability. In future, the continuous research of machine learning and deep learning will promote further development of remote sensing inversion technology. Remote sensing is a very helpful technique for evaluating macronutrients, such as SOC. The current study was based on the modeling of relationship between the spectral response and the concentrations of laboratory-estimated soil organic carbon (SOC_A). In detail, the linear regression models were applied to the reflectance spectra scanned by S2A and L8 images on the top soil of agricultural fields in the Al-Kharj region for the prediction of SOC. In summary, results from our investigations pointed out that the red and near-infrared regions are the most sensitive portions of the spectrum to SOC.

More specifically, the SWIR-1 band was found to be the most acceptable band for the prediction of SOC for both L8 (R^2 = 0.86) and S2A (R^2 = 0.77) satellites with BIAS of 16% and 14%, respectively. In case of vegetation indices, the BSI (R^2 = 0.79) and NDVI (R^2 = 0.72) for L8 images and BSI (R^2 = 0.86) and RSR (R^2 = 0.81) for S2A images were found to be good SOC predictors with a bias ranging between 11% and 16%. Moreover, the variation in the spectral bandwidth of L8 and S2A played an important role in

the selection of spectral indices. In particular, S2A bands produced an overall accuracy of 81% compared to 74% produced by L8 bands. Overall, the results of this study supported the hypothesis that L8 and S2A datasets could be beneficial for continuous monitoring of SOC. However, the derived empirical equations/models for the prediction of SOC were sensor-dependent. In other words, a regression developed for one sensor may not be applicable, at least without further study, to another instrument.

Acknowledgments

The authors are grateful to the Deanship of Scientific Research, King Saud University, Riyadh for funding this study through the Vice Deanship of Scientific Research Chairs. The unstinted cooperation and support extended by the staff of the Tawdeehiya Farms during the field campaign are gratefully acknowledged.

Add-on Information

Authors' contribution: R. Madugundu, K.A. Al-Gaadi, E. Tola: Contributed equally to conceptualization, preparation and implementation of the research work, field data collection and interpretation, analysis and modeling of satellite imagery, manuscript development and review, and follow-up of the publication process; **M. Edrris, H. Edrees, A. Alameen and R.B. Fulleros:** Contributed in taking and analyzing soil samples, assist in analyzing satellite images and statistical analysis of data.

Research content: The research content of manuscript is original and has not been published elsewhere.

Ethical approval: Not applicable

Conflict of interest: The authors declare that there is no conflict of interest.

Data from other sources: Not applicable

Consent to publish: All authors agree to publish the paper in *Journal of Environmental Biology*.

References

Bartholomeus, H., K. Lammert, S. Antoine, L. Martin, W. Bas, B. Eyal and T. Bernard: Soil organic carbon mapping of partially vegetated agricultural fields with imaging spectroscopy. *Int. J. Appl. Earth Obs. Geoinf.*, **13**, 81-88 (2011).

Baruah, R., B.K. Medhi and D. Bhattacharyya: Soil organic carbon storage and factors affecting its distribution in paddy and forest soil of Jorhat District of Assam. *J. Environ. Biol.,* **41**, 1798-1810 (2020).

Ben-Dor, E. and A. Banin: Near-infrared analysis as a rapid method to simultaneously evaluate several soil properties. *Soil Sci. Soc. Amer. J.,* **59**, 364-372 (1995).

Bhunia, G.S, P.K. Shit and H.R. Pourghasemi: Soil organic carbon mapping using remote sensing techniques and multivariate regression model. *Geocarto Int.,* **34**, 215-226 (2019).

Bhunia, G.S., P.K. Shit and R. Maiti: Comparison of GIS-based interpolation methods for spatial distribution of soil organic carbon (SOC). *J. Saudi Soc. Agric. Sci.,* **17**, 114-126 (2016).

Bouasria, A., K.I. Namr, A. Rahimi and E. M. Ettachfini: Soil organic matter estimation by using Landsat-8 pansharpened image and machine learning. In: 2020 Fourth International Conference on Intelligent Computing in Data Sciences (ICDS), 2020, pp. 1-8, doi: 10.1109/ICDS50568.2020.9268725.

Brown, L., J.M. Chen, S.G. Leblanc and J. Cihlar: A Shortwave Infrared modification to the simple ratio for LAI retrieval in Boreal Forests: An image and model analysis. *Remote Sens. Environ.,* **71**, 16-25 (2000).

Castaldi, F., A. Hueni, S. Chabrillat, K. Ward, G. Buttafuoco, B. Bomans, K. Vreys, M. Brell and B.V. Wesemael: Evaluating the capability of the Sentinel 2 data for soil organic carbon prediction in croplands. ISPRS *J. Photogramm. Remote Sens.,* **147**, 267–282 (2019).

Darwish, T. and A. Fadel: Mapping of soil organic carbon stock in the Arab countries to mitigate land degradation. *Arab. J. Geosci.,* **10**, 474 (2017).

De Pauw, E.: An agroecological exploration of the Arabian Peninsula. International Center for Agricultural Research in the Dry Areas (ICARDA), Aleppo, Syria, 77pp. (2002).

Dvorakova, K., U. Heiden and B. van Wesemael: Sentinel-2 Exposed Soil Composite for Soil Organic Carbon Prediction. *Remote Sens.,* **13**, 1791 (2021). https://doi.org/ 10.3390/rs13091791

Eitel, J.U.H., L.A. Vierling, M.E. Litvak, D.S. Long, U. Schulthess, A.A. Ager, D.J. Krofcheck and L. Stoscheck: Broadband, red-edge information from satellites improves early stress detection in a New Mexico conifer woodland. *Remote Sens. Environ.,* **115**, 3640-3646 (2011).

Huete, A., K. Didan, T. Miura, E.P. Rodriguez, X. Gao and L.G. Ferreira: Overview of the radiometric and biophysical performance of the MODIS vegetation indices. *Remote Sens. Environ.,* **83**, 195-213 (2016).

Ismail, M. and R.K. Yacoub: Digital soil map using the capability of new technology in sugar beet area, Nubariya, Egypt. *Egyptian J. Remote Sens. Space Sci.,* **15**, 113-124 (2012).

Jaber, S.M., C.L. Lant and M.I. Al-Qinna: Estimating spatial variations in soil organic carbon using satellite hyperspectral data and map algebra. *Int. J. Remote Sens.,* **32**, 5077-5103 (2012).

Jamalabad, M.S. and A.A. Akbar: Forest canopy density monitoring, using satellite images. In: Proceedings of the 20th ISPRS Congress, (Ed.: O. Altan). Commission VII, pp. 244–249 (2004).

Kooistra, L., J. Wanders, G.F. Epema, R.S.E.W. Leuven, R. Wehrens and L.M.C. Buydens: The potential of field scpectroscopy for the assessment of sediment properties in river floodplains. *Analytica Chimica Acta,* **484**, 198-200 (2003).

Kumar, P., P.C. Pandey, B.K. Singh, S. Katiyar, V.P. Mandal, M. Rani, V. Tomar and S. Patairiya: Estimation of accumulated soil organic carbon stock in tropical forest using geospatial strategy. *Egyptian J. Remote Sens. Space Sci.,* **19**, 109-123 (2016).

Lal, R.: Soil carbon sequestration impacts on global climate change and food security. *Science*, **304**, 1623-1627 (2004).

Mallick, J., M. Ahmed, S.D. Alqadhi, I.I. Falqi, M. Parayangat, C.K. Singh, A. Rahman and T. Ijyas: Spatial stochastic model for predicting soil organic matter using remote sensing data. *Geocarto Int.,* (2020), DOI:10.1080/10106049.2020.1720314

Man, W., H. Yu, L. Li, M. Liu, D. Mao, C. Ren, Z. Wang, M. Jia, Z. Miao, C. Lu and H. Li: Spatial expansion and soil organic carbon storage changes of croplands in the Sanjiang Plain, China. *Sustainability*, **9**, 563 (2017).

Mohamed, E.S., A.A El Baroudy, T. El-beshbeshy, M. Emam, A.A. Belal,

A. Elfadaly, A.A. Aldosari, A.M. Ali and R. Lasaponara: Vis-NIR spectroscopy and satellite Landsat-8 OLI Data to map soil nutrients in arid conditions: A case study of the North-west Coast of Egypt. *Remote Sens.,* **12**, 3716 (2020).

Mondal, A., D. Khare, S. Kundu, S. Mondal, S. Mukherjee and A. Mukhopadhyay: Spatial soil organic carbon (SOC) prediction by regression kriging using remote sensing data. *Egyptian J. Remote Sens. Space Sci.,* **20**, 67-70 (2017).

Nabiollahi, K., R. Taghizadeh-Mehrjardi and S. Eskandari: Assessing and monitoring the soil quality of forested and agricultural areas using soil-quality indices and digital soil-mapping in a semi-arid environment. *Arch. Agron. Soil Sci.,* **64**, 696–707 (2018).

Rosero-Vlasova, O.A., D. Borini-Alves, L. Vlassova, R. MontorioLlovería and F. Pérez-Cabello: Modeling soil organic matter (SOM) from satellite data using VISNIR-SWIR spectroscopy and PLS regression with step-down variable selection algorithm: Case study of Campos Amazonicos National Park savanna enclave, Brazil. In: Proceedings of the Remote Sensing for Agriculture, Ecosystems, and HydrologyXIX, Warsaw, Poland (Eds.: C.M. Neale and A. Maltese), SPIE: Bellingham, WA, USA., **Vol.** 10421, 64 p. (2017).

Rouse, Jr. J.W., R.H. Haas, J.A. Schell and D.W. Deering: Monitoring vegetation systems in the great plains with ERTS. Third Earth Resources Technology Satellite-1 Symposium, pp. 309-317, NASA, Washington, DC (1934).

Schillaci, C., L. Lombardo, S. Saia, M. Fantappie, M. Marker and M. Acutis: Modelling the topsoil carbon stock of agricultural lands with the Stochastic Gradient Treeboost in a semi-arid Mediterranean region. *Geoderma*, **286**, 35-45 (2017).

Schoonover, J. E. and J.F. Crim: An introduction to soil concepts and the role of soils in watershed management. *J. Contemp. Water Res. Edu.,* **154**, 21-47 (2015).

Shibu, M.E., P.A. Leffelaar, H. van Keulen and P.K. Aggarwal: Quantitative description of soil organic matter dynamics – A review of approaches with reference to rice-based cropping systems. *Geoderma,* **137**, 1-18 (2006).

Shit, P.K., G.S. Bhunia and R. Maiti.: Spatial analysis of soil properties using GIS based geostatistics models. *Model Earth Syst. Environ.,* **2**, 1-6 (2016).

Stevens, A., M. Nocita, G. Toth, L. Montanarella and B. van Wesemael: Prediction of soil organic carbon at the European Scale by visible and near infra red reflectance Spectroscopy. *PLoS ONE,* **8**, e66409 (2013).

Stoner, E.R. and M.F. Baumgardner: Characteristic variations in reflectance of surface soils. *Soil Sci. Soc. Amer. J.,* **45**, 1161-1165 (1981).

Tola, E., K.A. Al-Gaadi and R. Madugundu: Employment of GIS techniques to assess the long-term impact of tillage on the soil organic carbon of agricultural fields under hyper-arid conditions. *PLoS ONE*, **14**, e0212521, (2019).

Tola, E., K.A. Al-Gaadi, R. Madugundu, A.G. Kayad, A.A. Alameen, H.F. Edrees and M.K. Edrris: Determining soil organic carbon concentration in agricultural fields using a handheld spectroradiometer: Implication for soil fertility measurement. *Int. J. Agric. Biol. Engg.,* **11**, 13-19 (2018).

Viscarra-Rossel, R.A. and J. Bouma: Soil sensing: A new paradigm for agriculture. *Agric. Syst.,* **148**, 71-74 (2016).

Walkley, A. and I.A. Black: An examination of the Degtjareff method for determining soil organic matter and a proposed modification of the chromic acid titration method. *Soil Sci.,* **37**, 29-38 (1934).

Wang, B., C. Waters, S. Orgill, A. Cowie, A. Clark, D.L. Liu, M. Simpson, I. McGowen and T. Sides: Estimating soil organic carbon stocks using different modelling techniques in the semi-arid rangelands of eastern Australia. *Ecol. Indic.,* **88**, 425–438 (2018).

Wang, K., Y. Qi, W. Guo, J. Zhang and Q. Chang: Retrieval and mapping of soil organic carbon using Sentinel-2A spectral images from bare cropland in autumn. *Remote Sens.,* **13**,1072 (2021).

Zhou, T., Y. Geng, C. Ji, X. Xu, H. Wang, J. Pan, J. Bumberger, D. Haase and A. Lausch: Prediction of soil organic carbon and the C:N ratio on a national scale using machine learning and satellite data: A comparison between Sentinel-2, Sentinel-3 and Landsat-8 images. *Sci. Total Environ.,* **755**, 142661 (2021).